

THERMAL HADRON PRODUCTION
IN RELATIVISTIC NUCLEAR COLLISIONS*

A. ANDRONIC

GSI Helmholtzzentrum für Schwerionenforschung
64291 Darmstadt, Germany

P. BRAUN-MUNZINGER

ExtreMe Matter Institute EMMI
GSI Helmholtzzentrum für Schwerionenforschung
64291 Darmstadt, Germany
and
Technical University Darmstadt, 64289 Darmstadt, Germany

J. STACHEL

Physikalisches Institut der Universität Heidelberg
69120 Heidelberg, Germany*(Received February 18, 2009)*

We present the status of the description of hadron production in central nucleus–nucleus collisions within the statistical model. Extending previous studies by inclusion of very high-mass resonances ($m > 2$ GeV), and the up-to-now neglected scalar σ meson leads to an improved description of the data. In particular, the hitherto poorly reproduced energy dependence of the K^+/π^+ ratio at SPS energies (“the horn”) is now well described through the connection to the hadronic mass spectrum and, implicitly, Hagedorn’s limiting temperature.

PACS numbers: 25.75.Dw, 25.75.Nq

1. Introduction

One of the major goals of ultrarelativistic nuclear collision studies is to obtain information on the QCD phase diagram [1]. A promising approach is the investigation of hadron production. Hadron yields measured in central heavy ion collisions from AGS up to RHIC energies can be described very

* Presented at the IV Workshop on Particle Correlations and Femtoscopy, Kraków, Poland, September 11–14, 2008.

well [2–14] within a hadro-chemical equilibrium model. In our approach [2, 4, 7, 12] the only parameters are the chemical freeze-out temperature T and the baryo-chemical potential μ_b (and the fireball volume V , in case yields rather than ratios of yields are fitted); for a review see [15].

The main result of these investigations was that the extracted temperature values rise rather sharply from low energies on towards $\sqrt{s_{\text{NN}}} \simeq 10$ GeV and reach afterwards constant values near $T = 160$ MeV, while the baryochemical potential decreases smoothly as a function of energy. The limiting temperature [16] behavior suggests a connection to the phase boundary and it was, indeed, argued [17] that the quark–hadron phase transition drives the equilibration dynamically, at least for SPS energies and above. Considering also the results obtained for elementary collisions, where similar analyses of hadron multiplicities, albeit with several additional, non-statistical parameters (see [18, 19] and references therein), yield also temperature values in the range of 160 MeV, alternative interpretations were put forward. These include conjectures that the thermodynamical state is not reached by dynamical equilibration among constituents but rather is a generic fingerprint of hadronization [20, 21], or is a feature of the excited QCD vacuum [22]. The results presented below lend further support to the interpretation that the phase boundary is reflected in features of the hadron yields.

While in general all hadron yields are described rather quantitatively, a notable exception was up-to-now the energy dependence of the K^+/π^+ ratio which exhibits a rather marked maximum, “the horn” [25], near $\sqrt{s_{\text{NN}}} \simeq 10$ GeV [23]. Predicted first within a model of quark–gluon plasma (QGP) formation [25], the existence of such a maximum was also predicted [24] within the framework of the statistical model, but the observed rather sharp structure could not be reproduced [12]. Other attempts to describe the energy dependence of the K^+/π^+ ratio within the thermal model [11, 14] were also not successful, except when an energy-dependent light quark fugacity was used as an additional parameter [14]. Furthermore, all attempts to reproduce this structure within the framework of hadronic cascade models also failed, as is discussed in detail in [23]. As a consequence, the horn structure is taken in [23] as experimental evidence for the onset of deconfinement and QGP formation, and as support for the predictions of [25]. We have recently shown [30] that, employing an improved hadronic mass spectrum, in which the σ meson [29] and many higher-lying resonances are included, leads to an increase of about 16% for the calculated pion yields. This increase levels off near the point where the temperature reaches its limiting value, thereby sharpening the structure in the K^+/π^+ ratio, as will be shown below. For the Λ hyperons, the new high mass resonances lead to an increase in the calculated production of about 22%. An increase of up to 6% is observed for protons, while for kaons this increase is about 7%.

In Fig. 1 we present a comparison of measured and calculated hadron yields at the energies of $\sqrt{s_{\text{NN}}} = 7.6$ GeV (beam energy of 30 A GeV at SPS) and $\sqrt{s_{\text{NN}}} = 200$ GeV. The model is successful in reproducing the measurements and this applies to all energies, from 2 A GeV beam energy (fixed target) up to the top RHIC energy of $\sqrt{s_{\text{NN}}} = 200$ GeV. The reduced χ^2 values are reasonable. In most cases the fit quality is improved compared to our earlier analysis [12], even though the experimental errors are now smaller. A disagreement between the experiments is seen at the top RHIC energy for pions and protons, see Fig. 1, which is the reason of the large reduced χ^2 . A fit of ratios is in this case more suited, but we note that a fit of the STAR yields alone gives $T = 162$ MeV, $\mu_b = 32$ MeV, $V = 2400$ fm³, with a very good $\chi^2/N_{\text{df}} = 9.0/11$. The resonances were not included in the fits, but are quite well reproduced by the model.

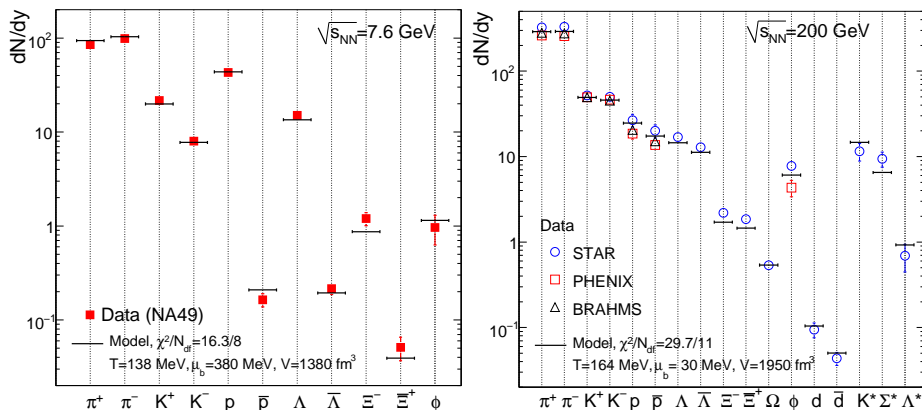


Fig. 1. Experimental hadron yields and model calculations for the parameters of the best fit at the energies of 7.6 (left panel) and 200 GeV (right panel; the Ω yield includes both Ω^- and $\bar{\Omega}^+$).

An important result of our analysis is that the resulting thermal parameters are close to those obtained earlier [12] and are in agreement with other recent studies [13, 28]. This indeed confirms that the common practice of including in the thermal codes hadrons up to masses of 2 GeV (for instance in the publicly-available code THERMUS [31]) does not lead to significantly biased fit parameters. Nevertheless, there are small variations. In Fig. 2 we present the energy dependence of T and μ_b in comparison to our earlier results [12]. We have parametrized T as a function of $\sqrt{s_{\text{NN}}}$ with the following expression¹:

¹ For μ_b , there is no need to change our earlier [12] parametrization: $\mu_b[\text{MeV}] = \frac{1303}{1+0.286\sqrt{s_{\text{NN}}(\text{GeV})}}$.

$$T = T_{\text{lim}} \frac{1}{1 + \exp(2.60 - \ln(\sqrt{s_{\text{NN}}}(\text{GeV}))/0.45)}, \quad (1)$$

with the “limiting” temperature $T_{\text{lim}} = 164$ MeV. This value is slightly higher compared to our earlier value of 161 ± 4 MeV [12] due to the higher temperatures presently derived for the RHIC energies. The approach to T_{lim} is presently more gradual compared to our earlier parametrization.

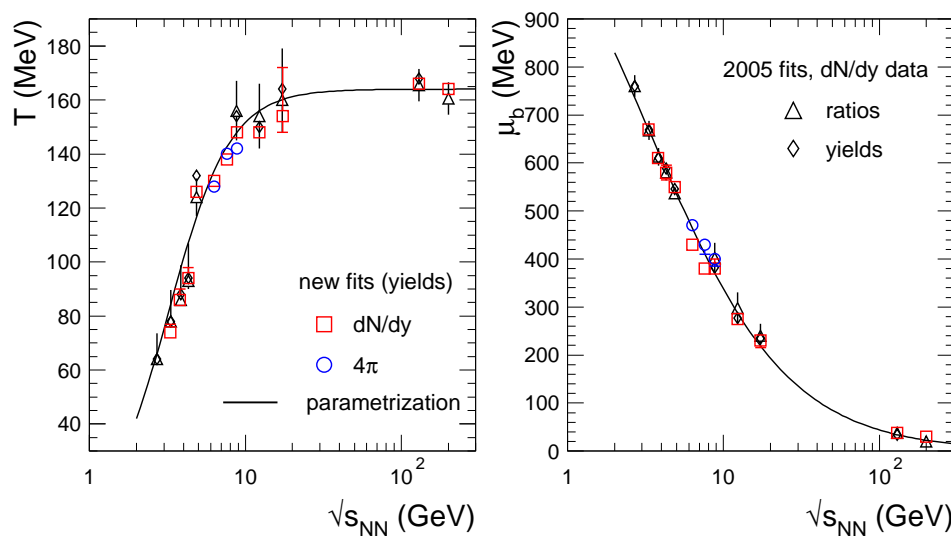


Fig. 2. The energy dependence of the temperature and baryon chemical potential at chemical freeze-out. The results of the new fits [30] are compared to the values obtained in our earlier study [12]. The lines are parametrizations for T and μ_b (see text).

The values of μ_b extracted for the two lowest SPS energies deviate somewhat from the continuous trend suggested by all the other points. At these energies the fit to data in full phase space does lead, as expected, to larger values of μ_b , which do fit in the systematics. At 40 A GeV ($\sqrt{s_{\text{NN}}} = 8.8$ GeV) the resulting values of T and μ_b from the fit of 4π data are very similar to those obtained from midrapidity data.

The volume at chemical freeze-out (corresponding to a slice of one unit of rapidity, dV/dy) is shown in Fig. 3 as a function of energy. The values extracted directly from the fits of particle yields are compared to the values obtained by dividing the measured charged particle rapidity densities with densities calculated employing the above parametrizations of T and μ_b . As expected, the two methods give very similar results. The chemical freeze-out volume is compared to the kinetic freeze-out volume extracted from

Hanbury-Brown and Twiss (HBT) measurements, V_{HBT} [32]. Note that, to relate quantitatively the magnitude of the rapidity density of the chemical freeze-out volume dV/dy to the volume at kinetic freeze-out determined from HBT measurements, one needs to map rapidity onto space (see the discussion in [32]). Here we only observe that the energy dependence of the two observables exhibit a similar non-monotonic behavior. It is interesting to note that the minimum of dV/dy occurs at the $\sqrt{s_{\text{NN}}}$ corresponding to the saturation of T .

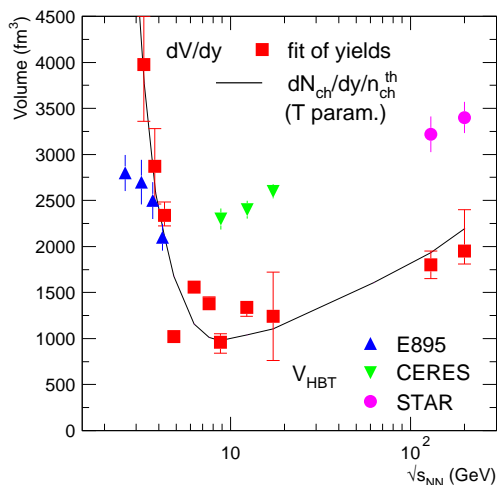


Fig. 3. The fireball volume at chemical freeze-out compared to the volume extracted from the HBT measurements [32].

We employ the above parametrizations of T and μ_b to investigate the energy dependence of the production yields of various hadrons relative to pions, shown in Fig. 4. In particular, the K^+/π^+ ratio shows a rather pronounced maximum at a beam energy of 30 A GeV [23], and the data are well reproduced by the model calculations. In the thermal model this maximum occurs naturally at $\sqrt{s_{\text{NN}}} \simeq 8$ GeV [24]. It is due to the counteracting effects of the steep rise and saturation of T and the strong monotonous decrease in μ_b . The competing effects are most prominently reflected in the energy dependence of the Λ hyperon to pion ratio (right panel of Fig. 4), which shows a pronounced maximum at $\sqrt{s_{\text{NN}}} \simeq 5$ GeV. This is reflected in the K^+/π^+ ratio somewhat less directly; it appears mainly as a consequence of strangeness neutrality, assumed in our calculations.

The model describes the K^+/π^+ data very well over the full energy range, as a consequence of the inclusion in the code of the high-mass resonances and of the σ meson, while our earlier calculations [12] were overpredicting the SPS data. At RHIC energies, the quality of the present fits is essentially

unchanged compared to [12], as also the data have changed somewhat. The model also describes accurately the Λ/π^- measurements as well as those for other hyperons. We note that the maxima in the various production ratios are located at different energies [34]. The model calculations reproduce this feature in detail.

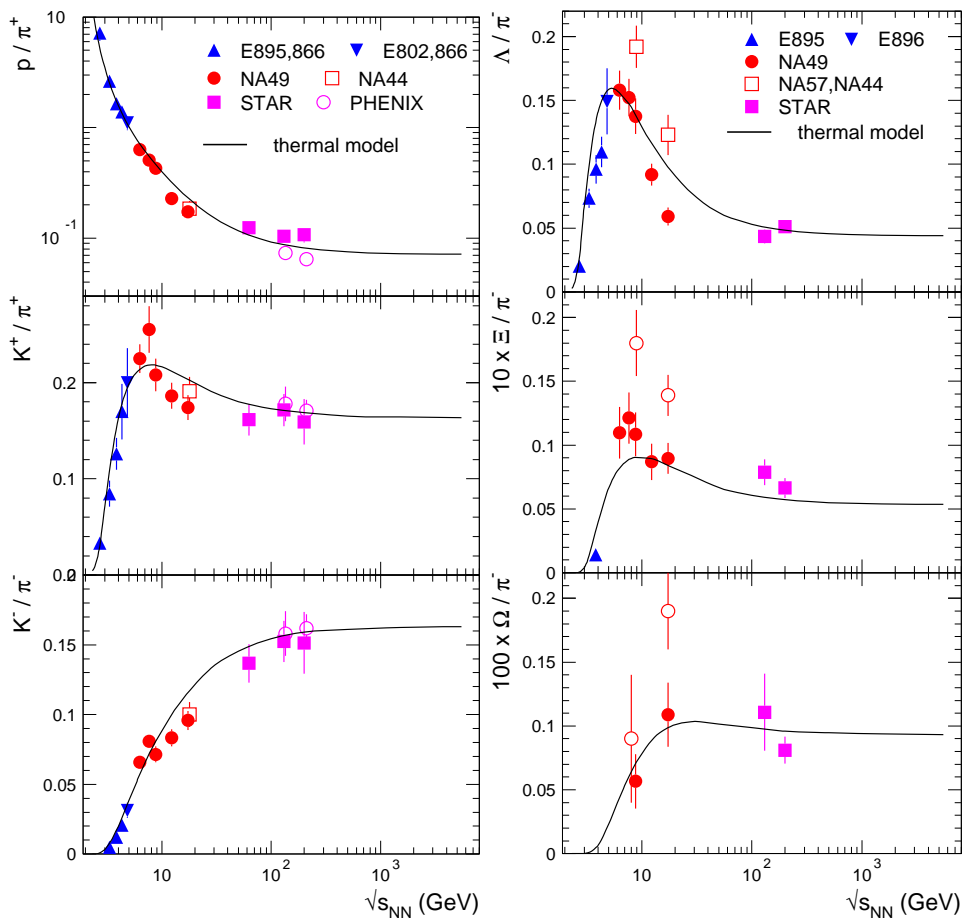


Fig. 4. Energy dependence of hadron yields relative to pions.

The calculated K^+/π^+ ratio is likely to decrease further at energies beyond the maximum and the peak is likely to sharpen somewhat [30] if our presumably still incomplete knowledge of the hadronic spectrum for masses larger than 2 GeV would improve. The uncertainty of the calculations due to the mass and width of the σ meson are at the percent level only. Another few percent uncertainty, which is difficult to assess quantitatively, arises from the unknown branching ratios of the high-mass resonances.

In summary, our results [30] demonstrate that by inclusion of the σ meson and many higher mass resonances into the resonance spectrum employed in the statistical model calculations an improved description is obtained of hadron production in central nucleus–nucleus collisions at ultra-relativistic energies. A dramatic improvement is visible for the K^+/π^+ ratio, which is now well described at all energies. The “horn” finds herewith a natural explanation which is, however, deeply rooted in and connected to detailed features of the hadronic mass spectrum which leads to a limiting temperature and contains the QCD phase transition [16]. Our results strongly imply that hadronic observables near and above the horn structure at a beam energy of 30 A GeV provide a link to the QCD phase transition. Open questions are whether the chemical freeze-out curve below the horn energy actually traces the QCD phase boundary at large values of chemical potential or whether chemical freeze-out in this energy range is influenced by exotic new phases such as have been predicted in [35]. In any case these are exciting prospects for new physics to be explored at RHIC low energy runs and, in particular, at the high luminosity FAIR facility. At the high energy frontier, the measurements at LHC will be a crucial test of the present picture.

We acknowledge the support from the Alliance Program of the Helmholtz-Gemeinschaft.

REFERENCES

- [1] P. Braun-Munzinger, J. Wambach, [arXiv:0801.4256 \[hep-ph\]](#), submitted to *Rev. Mod. Phys.*
- [2] P. Braun-Munzinger, J. Stachel, J.P. Wessels, N. Xu, **B344**, 43 (1995) [[nucl-th/9410026](#)]; *Phys. Lett.* **B365**, 1 (1996) [[nucl-th/9508020](#)].
- [3] J. Cleymans, D. Elliott, H. Satz, R.L. Thews, *Z. Phys.* **C74**, 319 (1997) [[nucl-th/9603004](#)].
- [4] P. Braun-Munzinger, I. Heppe, J. Stachel, *Phys. Lett.* **B465**, 15 (1999) [[nucl-th/9903010](#)].
- [5] J. Cleymans, K. Redlich, *Phys. Rev.* **C60**, 054908 (1999) [[nucl-th/9903063](#)].
- [6] F. Becattini, J. Cleymans, A. Keranen, E. Suhonen, K. Redlich, *Phys. Rev.* **C64**, 024901 (2001) [[hep-ph/0002267](#)].
- [7] P. Braun-Munzinger, D. Magestro, K. Redlich, J. Stachel, *Phys. Lett.* **B518**, 41 (2001) [[hep-ph/0105229](#)].
- [8] N. Xu, M. Kaneta, *Nucl. Phys.* **A698**, 306c (2002).
- [9] F. Becattini, *J. Phys. G* **28**, 1553 (2002).
- [10] R. Rapp, E. Shuryak, *Phys. Rev. Lett.* **86**, 2980 (2001) [[hep-ph/0008326](#)].
- [11] F. Becattini, M. Gaździcki, J. Manninen, *Phys. Rev.* **C73**, 044905 (2006) [[hep-ph/0511092](#)].

- [12] A. Andronic, P. Braun-Munzinger, J. Stachel, *Nucl. Phys.* **A772**, 167 (2006) [[nucl-th/0511071](#)].
- [13] J. Manninen, F. Becattini, *Phys. Rev.* **C78**, 054901 (2008) [[arXiv:0806.4100](#)] [[nucl-th](#)].
- [14] J. Letessier, J. Rafelski, *Eur. Phys. J.* **A35**, 221 (2008) [[nucl-th/0504028](#)].
- [15] P. Braun-Munzinger, K. Redlich, J. Stachel, [nucl-th/0304013](#), invited review in *Quark Gluon Plasma 3*, eds. R.C. Hwa, X.N. Wang, World Scientific Publishing, 2004.
- [16] R. Hagedorn, CERN-TH-4100/85 (1985).
- [17] P. Braun-Munzinger, J. Stachel, C. Wetterich, *Phys. Lett.* **B596**, 61 (2004) [[nucl-th/0311005](#)].
- [18] A. Andronic, F. Beutler, P. Braun-Munzinger, K. Redlich, J. Stachel, [arXiv:0804.4132](#) [[hep-ph](#)].
- [19] F. Becattini, P. Castorina, J. Manninen, H. Satz, [arXiv:0805.0964](#) [[hep-ph](#)].
- [20] R. Stock, *Phys. Lett.* **B465**, 277 (1999) [[hep-ph/9905247](#)].
- [21] U. Heinz, *Nucl. Phys.* **A685**, 414 (2001) [[hep-ph/0009170](#)].
- [22] P. Castorina, D. Kharzeev, H. Satz, *Eur. Phys. J.* **C52**, 187 (2007) [[arXiv:0704.1426](#)] [[hep-ph](#)].
- [23] C. Alt *et al.* [NA49 Collaboration], *Phys. Rev.* **C77**, 024903 (2008) [[arXiv:0710.0118](#)] [[nucl-ex](#)].
- [24] P. Braun-Munzinger, J. Cleymans, H. Oeschler, K. Redlich, *Nucl. Phys.* **A697**, 902 (2002) [[hep-ph/0106066](#)].
- [25] M. Gaździcki, M.I. Gorenstein, *Acta Phys. Pol. B* **30**, 2705 (1999) [[hep-ph/9803462](#)].
- [26] C. Alt *et al.* [NA49 Collaboration], *Phys. Rev.* **C78**, 034918 (2008) [[arXiv:0804.3770](#)] [[nucl-ex](#)].
- [27] C. Alt *et al.* [NA49 Collaboration], *Phys. Rev.* **C78**, 044908 (2008) [[arXiv:0806.1937](#)] [[nucl-ex](#)].
- [28] B.I. Abelev *et al.* [STAR Collaboration], [arXiv:0808.2041](#) [[nucl-ex](#)].
- [29] R. García-Martín, J.R. Peláez, F.J. Ynduráin, *Phys. Rev.* **D76**, 074034 (2007) [[hep-ph/0701025](#)].
- [30] A. Andronic, P. Braun-Munzinger, J. Stachel, [arXiv:0812.1186](#) [[nucl-th](#)].
- [31] S. Wheaton, J. Cleymans, *Comput. Phys. Commun.* **180**, 84 (2009) [[hep-ph/0407174](#)].
- [32] D. Adamova *et al.* [CERES Collaboration], *Phys. Rev. Lett.* **90**, 022301 (2003) [[nucl-ex/0207008](#)]; for a review, see M. Lisa, S. Pratt, R. Soltz, U. Wiedemann, *Ann. Rev. Nucl. Part. Sci.* **55**, 357 (2005) [[nucl-ex/0505014](#)].
- [33] J. Steinheimer *et al.*, [arXiv:0811.4077](#) [[hep-ph](#)].
- [34] J. Cleymans, H. Oeschler, K. Redlich, S. Wheaton, *Phys. Lett.* **B615**, 50 (2005) [[hep-ph/0411187](#)].
- [35] L. McLerran, R. Pisarski, *Nucl. Phys.* **A796**, 83 (2007) [[arXiv:0706.2191](#)] [[hep-ph](#)].